RESEARCH

Energy-efficient power control for contention-based synchronization in OFDMA systems with discrete powers and limited feedback

Giacomo Bacci[1,2*], Luca Sanguinetti[2], Marco Luise[2] and Harold Vincent Poor[1]

Abstract

This work derives a distributed and iterative algorithm by which mobile terminals can selfishly control their transmit powers during the synchronization procedure specified by the IEEE 802.16 m and the 3GPP long-term evolution standards for orthogonal frequency-division multiple-access technologies. The proposed solution aims at maximizing the energy efficiency of the network and is derived on the basis of a finite noncooperative game in which the players have discrete action sets of transmit powers. The set of Nash equilibria of the game is investigated, and a distributed power control algorithm is proposed to achieve synchronization in an energy-efficient manner under the assumption that the feedback from the base station is limited. Numerical results show that the proposed solution improves the energy efficiency as well as the timing estimation accuracy of the network compared to existing alternatives while requiring a reasonable amount of information to be exchanged on the return channel.

1 Introduction

The issue of energy efficiency has attracted considerable interest in the information and telecommunication technology community during the last decade, as witnessed by the extensive literature available on this subject (see, for example, [1] and references therein). Among others, a challenge that lies in this paradigm is to prolong the battery life of mobile terminals based on orthogonal frequency-division multiple-access (OFDMA) technologies such as those operating according to the IEEE 802.16 m [2] and the 3GPP long-term evolution (LTE) [3] standards. The first operation that must be accomplished by any terminal when joining the network is achieving correct synchronization with its serving base station (BS). This procedure is called initial ranging in IEEE 802.16 m [2] and random access in LTE [3]. It relies on a contention-based approach taking place over a specified set of subcarriers, which are used by each terminal to notify its entry request by transmitting a packet consisting of a randomly chosen code. Code identification as well as

multiuser timing estimation are the main tasks of the BS during this procedure. These problems have received significant attention in the past few years, and some solutions are currently available in the literature (see, for example, [4-7] and references therein). All the aforementioned works assume to increase the transmit power upon successful synchronization without taking into account any energy efficiency issue. This is motivated by the fact that the energy efficiency problem in OFDMA-based technologies has been mainly analyzed for the data transmission phase (see [8] and [9] and references therein). A first attempt to reduce the power consumption during the initial synchronization phase can be found in [10], in which a low-complexity and iterative algorithm is proposed to allow each synchronization terminal (ST) and the BS to locally choose the transmit power and the detection strategy, respectively. The goal is to obtain a good trade-off between detection capabilities and power consumption while satisfying quality-of-service (QoS) requirements given in terms of timing estimation error and probability of false code lock. The proposed solution is based on a noncooperative game-theoretic formulation, and it is shown to provide significant gains in terms of reduced synchronization time and parameter estimation accuracy

*Correspondence: giacomo.bacci@iet.unipi.it
[1] Department of Electrical Engineering, Princeton University, Olden Street, Princeton, NJ 08544, USA
[2] Dip. Ingegneria dell'Informazione, University of Pisa, Via Caruso, Pisa 56126, Italy

compared to existing alternatives based on a deterministic increase of the transmit power. Although interesting from a theoretical point of view, the analysis provided in [10] is not suited for practical applications since it relies on the assumption of a continuous set of transmit powers. Moreover, comparisons with existing alternatives are carried out assuming that STs have perfect knowledge of the signal-to-interference-plus-noise ratio (SINR) measured at the BS. A similar game-theoretic line of reasoning has been recently used for achieving synchronization in code-division multiple-access networks operating in a flat-fading scenario [11,12] and in a frequency-selective one [13].

Motivated by the above considerations, in this work we return to the problem discussed in [10] and extend both the power allocation approach and the numerical analysis as follows. We first assume that a *finite* set of transmit powers is available at each terminal. Compared to [10], this more application-oriented assumption changes completely the nature of the energy-efficient optimization problem, as the tool of finite noncooperative game theory is used to find its solution [14]. The set of Nash equilibria of the game is investigated and compared to that of the continuous-power noncooperative game discussed in [10]. The theoretical analysis of the finite game is adopted to derive an iterative and distributed power allocation algorithm for achieving synchronization under the assumption of a *limited feedback* from the BS. Numerical results are used to compare the performance of the proposed solution with that achieved by existing alternatives based on a deterministic increase of the transmit power (with and without contention resolution methods). It turns out that the proposed solution provides benefits in terms of energy efficiency and parameter estimation accuracy, using a reasonable amount of feedback resources.

The remainder of this paper is structured as follows.[a] Section 2 describes the system model and introduces the problem. Section 3 formulates the game and investigates its equilibria. The analysis is used in Section 4 to derive an iterative and distributed synchronization algorithm whose performance is assessed by means of numerical results. Finally, Section 5 concludes the paper and discusses the applicability of this technique to current wireless standards.

2 System model and problem formulation

2.1 System model

We consider the uplink of an OFDMA-based system employing N subcarriers with index set $\{0, 1, \ldots, N-1\}$. To avoid aliasing problems, $2N_v$ null subcarriers are placed at the spectrum edges. The remaining $N - 2N_v$ subcarriers are grouped into synchronization subcarriers and data subcarriers. The former are used by the STs

entering the network through a *contention-based synchronization procedure*, while the latter are assigned to mobile terminals for data transmission and channel estimation. We denote by K the number of STs and assume that the synchronization subcarriers are divided into M sub-bands, each composed of a set of V adjacent subcarriers, which is called a *tile*. We denote by $\mathbf{c}_\ell = [c_\ell(0), c_\ell(1), \ldots, c_\ell(MV - 1)]$ the code chosen by the ℓth ST and call θ_ℓ the timing offset of the ℓth ST (normalized to the sampling period T_s).

As in [10], we consider a quasi-synchronous system in which no interblock interference is present at the BS receiver, and we neglect any residual carrier frequency offset.[b] Moreover, we assume that the channel frequency response is nearly flat over each tile and independent across tiles. In addition, users other than those performing synchronization have been successfully synchronized to the BS so that they do not generate significant interference. Under the above assumptions, the V- dimensional vector $\mathbf{X}(m)$ containing the mth-tile discrete Fourier transform outputs at the BS can be written as

$$\mathbf{X}(m) = \sum_{\ell=1}^{K} \sqrt{p_\ell}\,\mathbf{C}_\ell(m)\mathbf{a}(\theta_\ell)H_\ell(m) + \mathbf{n}(m) \ \text{ for}$$
$$m = 0, 1, \ldots, M-1 \tag{1}$$

where p_ℓ denotes the transmit power of the kth ST, $\mathbf{C}_\ell(m) = \text{diag}\{c_\ell(mV), \ldots, c_\ell(mV + V - 1)\}$, the vector $\mathbf{a}(\theta_\ell)$ is given by

$$\mathbf{a}(\theta_\ell) = [1, e^{-j2\pi\theta_\ell/N}, \ldots, e^{-j2\pi(V-1)\theta_\ell/N}]^T \tag{2}$$

and $\mathbf{n}(m)$ is the additive white Gaussian noise (AWGN) with zero mean and covariance matrix $\sigma_n^2 \mathbf{I}_V$.

As mentioned above, the main tasks of the BS during the synchronization procedure are code detection and timing offset estimation. This is achieved by exploiting the observation vectors $\{\mathbf{X}(m); m = 0, 1, \ldots, M-1\}$. Following [10], the kth code $\mathbf{c}_k$ is declared as detected if the following generalized likelihood ratio test (GLRT) is satisfied:

$$\frac{\Lambda_k(\hat{\theta}_k)}{\sum_{m=0}^{M-1} \|\mathbf{X}(m)\|^2} \geq \lambda \tag{3}$$

where the threshold λ is a design parameter chosen so as to achieve a desired probability of false alarm $\overline{\Pi}_{\text{fa}}$, and $\Lambda(\hat{\theta}_k)$ is given by

$$\Lambda(\hat{\theta}_k) = \frac{1}{V} \sum_{m=0}^{M-1} \left| \mathbf{a}^H(\hat{\theta}_k)\mathbf{C}_k^H(m)\mathbf{X}(m) \right|^2. \tag{4}$$

In the above equation, $\hat{\theta}_k$ is the maximum likelihood estimate of θ_k, given by [10]

$$\hat{\theta}_k = \arg \max_{0 \leq \tilde{\theta}_k \leq \overline{\theta}} \Lambda(\tilde{\theta}_k) \tag{5}$$

with $\overline{\theta}$ being the (normalized) round trip propagation delay for a user located at the cell boundary [15].

2.2 Problem formulation

Without loss of generality, we focus on the kth ST and rewrite the right-hand side of (1) as

$$\mathbf{X}(m) = \sqrt{p_k}\,\mathbf{C}_k(m)\mathbf{a}(\theta_k)H_k(m) + \mathbf{w}_k(m) \tag{6}$$

where

$$\mathbf{w}_k(m) = \sum_{\ell=1,\ell\neq k}^{K} \sqrt{p_\ell}\,\mathbf{C}_\ell(m)\mathbf{a}(\theta_\ell)H_\ell(m) + \mathbf{n}(m) \tag{7}$$

accounts for the contribution of the other STs plus thermal noise. To make the problem tractable, we model the channel frequency responses $H_\ell(m)$ for $m = 0, 1, \ldots, M-1$ experienced by the ℓth user across tiles as independent Gaussian random variables with zero means and powers $|H(m)|^2$. In these circumstances, the vector $\mathbf{w}_k = [\mathbf{w}_k(0), \mathbf{w}_k(1), \ldots, \mathbf{w}_k(M-1)]^T$ has zero mean and a variance given by

$$\sigma_{w_k}^2 = \sigma_n^2 + \sum_{\ell=1,\ell\neq k}^{K} \alpha_\ell p_\ell \tag{8}$$

where $\alpha_\ell = 1/M \sum_{m=0}^{M-1} |H_\ell(m)|^2$ is ST ℓ's average channel power gain across the tiles. To proceed further, we let $\mathbf{p} = [p_1, p_2, \ldots, p_K]^T$ and denote by γ_k the SINR of the kth ST over the observation vectors $\{\mathbf{X}(m); m = 0, 1, \ldots, M-1\}$. Using (8), from (6) it easily follows that γ_k takes the form [10]

$$\gamma_k = v_k(\mathbf{p}_{\backslash k})p_k \tag{9}$$

where $\mathbf{p}_{\backslash k} = \mathbf{p} \setminus p_k = [p_1, \ldots, p_{k-1}, p_{k+1}, \ldots, p_K]^T$, and $v_k(\mathbf{p}_{\backslash k})$ is defined as

$$v_k(\mathbf{p}_{\backslash k}) = \frac{V\alpha_k}{\sigma_{w_k}^2} = \frac{V\alpha_k}{\sigma_n^2 + \sum_{\ell\neq k}\alpha_\ell p_\ell}. \tag{10}$$

Following [10], the energy-efficient optimization problem can be mathematically formalized for all STs $k \in \mathcal{K} = \{1, \ldots, K\}$ as

$$p_k^\star = \arg \max_{p_k \in \mathcal{P}_k} \quad \frac{\Pi_{\mathrm{d},k}(\gamma_k)}{p_k T} \tag{11}$$

$$\text{subject to} \quad \mathrm{MSE}(\hat{\theta}_k) \leq \overline{\mathrm{MSE}}_\theta \tag{12}$$

where $\mathcal{P}_k$ denotes the set of transmit powers and T is the duration of the cyclically extended OFDMA block, whereas $\mathrm{MSE}(\hat{\theta}_k) = \mathbb{E}\{|\hat{\theta}_k - \theta_k|^2\}$ is the mean-square error (MSE) of the timing estimate $\hat{\theta}_k$, and $\overline{\mathrm{MSE}}_\theta$ is the network QoS requirement in terms of maximum timing estimation MSE. In addition, $\Pi_{\mathrm{d},k}(\gamma_k)$ represents the probability of correct detection of code $\mathbf{c}_k$ given by [10]

$$\Pi_{\mathrm{d},k}(\gamma_k) = I_{\frac{(1+\gamma_k)(1-\lambda)}{1+(1-\lambda)\gamma_k}} [M(V-1), M] \tag{13}$$

where $I_x[\cdot, \cdot]$ is the incomplete beta function [16]. Unlike [10], we assume that the power strategy set $\mathcal{P}_k$ is finite and given by

$$\mathcal{P}_k = \left\{ \pi_k^{(1)}, \pi_k^{(2)}, \ldots, \pi_k^{(Q_k)} \right\} \tag{14}$$

where the number of power levels Q_k is computed as

$$Q_k = 1 + \frac{\overline{p}_k \mid_{\mathrm{dB}} - \underline{p}_k \mid_{\mathrm{dB}}}{\Delta_k \mid_{\mathrm{dB}}} \tag{15}$$

with $\Delta_k > 1$ being the quantization step, and $\underline{p}_k$ and $\overline{p}_k$ denoting the minimum and maximum power levels, respectively, where $\overline{p}_k$ is assumed to be sufficiently large [17].[c] From (14) and (15), it follows that $\pi_k^{(1)} = \underline{p}_k$, $\pi_k^{(Q_k)} = \overline{p}_k$, and $\pi_k^{(q)} = \underline{p}_k \cdot \Delta_k^{q-1}$.

Setting $\mathcal{P}_k$ as specified in (14) allows us to meet the technical requirements of practical systems in which transmit powers are usually equally spaced on a logarithmic scale to reduce the complexity of the front-end architecture and to increase the efficiency of power amplifiers (see, for example, the specifications provided by the IEEE 802.16 m and 3GPP LTE standards in [2] and [3], respectively). For simplicity, in all subsequent derivations, we assume that $\Delta_k = \Delta$, $\underline{p}_k = \underline{p}$, and $\overline{p}_k = \overline{p}$ for all $k \in \mathcal{K}$. This also implies that $Q_k = Q$.

As mentioned previously, the aim of this work is to solve (11) taking into account the discrete nature of the power strategy sets $\{\mathcal{P}_k\}$. In the sequel, this is achieved by resorting to the analytical tools of finite game theory [14].

3 Game formulation and analysis

Using the results illustrated in [10], it follows that the MSE in (12) can be met provided that

$$p_k \geq \frac{\gamma_{\mathrm{req}}}{v_k(\mathbf{p}_{\backslash k})} \tag{16}$$

where γ_{req} denotes the minimum SINR such that the MSE constraint (12) is satisfied with equality, i.e., $\mathrm{MSE}(\hat{\theta}_k) = \overline{\mathrm{MSE}}_\theta$. In particular, γ_{req} is found to be [10]

$$\gamma_{\mathrm{req}} = \frac{3N^2}{2M\pi^2(V^2-1)} \cdot \frac{1}{\rho} \tag{17}$$

where ρ is defined as $\rho = \overline{\mathrm{MSE}}_\theta - \mu^2(\hat{\theta}_k)$ with $\mu(\hat{\theta}_k) = \mathbb{E}\{\hat{\theta}_k\} - \theta_k$ denoting the bias of the timing estimate $\hat{\theta}_k$. Using (16), the optimization problem in (11) can be reformulated as

$$p_k^\star = \arg \max_{p_k \in \mathcal{A}_k(\mathbf{p}_{\backslash k})} \quad \frac{\Pi_{\mathrm{d},k}(\gamma_k)}{p_k T} \tag{18}$$

where

$$\mathcal{A}_k(\mathbf{p}_{\backslash k}) = \left\{ p_k \in \mathcal{P}_k : p_k \geq \frac{\gamma_{\mathrm{req}}}{v_k(\mathbf{p}_{\backslash k})} \right\} \tag{19}$$

is the power strategy subset that allows the kth ST to meet the MSE constraint in (11). For notational simplicity, in all subsequent derivations, we omit the functional dependence of $\mathcal{A}_k$ on $\mathbf{p}_{\setminus k}$.

The power allocation problem in (18) can be formulated as a generalized[d] noncooperative game with complete information [14], denoted by $\mathcal{G} = [\mathcal{K}, \{\mathcal{A}_k\}, \{u_k\}]$. In particular, $\mathcal{K} = \{1, 2, \ldots, K\}$ is the player set, $\mathcal{A}_k$ is the action set of the kth player, and u_k is its payoff (utility) function given by

$$u_k(\mathbf{p}) = \frac{\Pi_{\mathrm{d},k}(\gamma_k)}{p_k T} \tag{20}$$

which depends on the power allocation $\mathbf{p}$ through γ_k as in (9). The discrete nature of $\mathcal{A}_k$ places $\mathcal{G}$ into the category of finite generalized noncooperative games. As mentioned previously, this is much different from [10], in which the *continuous* nature of the action sets allows us to formalize the optimization problem as an *infinite* generalized noncooperative game $\mathcal{G}_c$.

3.1 Analysis of the equilibria

The existence and uniqueness of the generalized Nash equilibria (GNE) of $\mathcal{G}$ are studied in the following. The analysis is conducted only for *pure* (i.e., deterministic) strategies. This choice is motivated by the fact that, in compact strategy spaces, *mixed* (i.e., statistical) strategies are generally less attractive due to (a) implementation difficulties in wireless communications systems [17], as they require the presence of an arbitrator in the network to properly coordinate the players, and (b) Pareto inferiority [14] of any mixed-strategy profiles to pure-strategy profiles [18] that reduces the total utility of the network.

To proceed further, we recall that a vector $\mathbf{p}^\star = [p_1^\star, p_2^\star, \ldots, p_K^\star]^T$ is a pure-strategy GNE of $\mathcal{G}$ if, for any $k \in \mathcal{K}$,

$$u_k\left([p_k^\star, \mathbf{p}_{\setminus k}^\star]\right) \geq u_k\left([p_k, \mathbf{p}_{\setminus k}^\star]\right) \tag{21}$$

for all transmit powers $p_k \in \mathcal{A}_k$. Another way to define a pure-strategy GNE is to make use of the concept of *best response* [14]. In particular, we have that a vector $\mathbf{p}^\star$ is a GNE if each element $p_k^\star$ is the best response $r_k(\mathbf{p}_{\setminus k}^\star)$ to the powers $\mathbf{p}_{\setminus k}^\star$ chosen by the other players, with $r_k(\mathbf{p}_{\setminus k}^\star)$ being the solution of the following problem:

$$r_k(\mathbf{p}_{\setminus k}^\star) = \arg \max_{\tilde{p}_k \in \mathcal{A}_k} \frac{\Pi_{\mathrm{d},k}(\nu_k(\mathbf{p}_{\setminus k}^\star)\tilde{p}_k)}{\tilde{p}_k T} \tag{22}$$

in which we have used (20), and we have explicitly written the functional dependence of the detection probability $\Pi_{\mathrm{d},k}$ on $\tilde{p}_k$ and $\mathbf{p}_{\setminus k}^\star$ through γ_k in (9).

Theorem 1. *Let us define the SINR $\gamma^\star$ as*

$$\gamma^\star = \max(\gamma_{\mathrm{req}}, \tilde{\gamma}) \tag{23}$$

with $\tilde{\gamma}$ being the solution of

$$\left.\frac{\partial \Pi_{\mathrm{d},k}(\gamma)}{\partial \gamma}\right|_{\gamma=\tilde{\gamma}} = \frac{\Pi_{\mathrm{d},k}(\tilde{\gamma})}{\tilde{\gamma}}. \tag{24}$$

Then, the game $\mathcal{G}$ admits pure-strategy GNE provided that

$$\gamma^\star(K - 1) < V. \tag{25}$$

The proof can be found in Appendix 1.

Theorem 2. *If condition (25) is satisfied, then the cardinality of the set $\mathcal{E}^\star$ of pure GNE for $\mathcal{G}$ is such that*

$$|\mathcal{E}^\star| \geq 1. \tag{26}$$

The proof can be found in Appendix 2.

Theorem 1 provides a *sufficient* condition for the set of GNE not to be empty,[e] and Theorem 2 states that the GNE is not necessarily unique. This means that the uniqueness property proven in [10] for $\mathcal{G}_c$ no longer holds for $\mathcal{G}$. In other words, quantizing the set of actions makes the game $\mathcal{G}$ lose the uniqueness property for the GNE. In this context, it is interesting to show the following result.

Theorem 3. *Among all $\mathbf{p}^\star \in \mathcal{E}^\star$, the smallest[f] GNE $\mathbf{p}_\Delta^\star$ is such that*

$$\mathbf{p}_\Delta^\star = \arg \max_{\mathbf{p}^\star \in \mathcal{E}^\star} \sum_{k=1}^{K} u_k(\mathbf{p}^\star). \tag{27}$$

The proof can be found in Appendix 3.

The above result states that $\mathbf{p}_\Delta^\star$ is the best GNE in terms of social welfare (joint optimization) or, equivalently, it is the most efficient GNE in a social sense [19]. Note that this does not amount to saying that $\mathbf{p}_\Delta^\star$ is the socially optimum solution of (11), as noncooperative equilibria are known to be generally inefficient [19]. Improving the equilibrium efficiency is out of the scope of this paper and is left as a future work.

3.2 Numerical analysis

Unlike the unique GNE of $\mathcal{G}_c$ in [10], the multiple equilibria of $\mathcal{G}$ cannot be expressed in a closed form as a function of the network parameters because of the 'arg max' operator in (22). A numerical analysis is thus conducted to make comparisons and to evaluate the impact of the discretization of the action sets. To this aim, we concentrate on the optimal (in a social sense) $\mathbf{p}_\Delta^\star$ and resort to the exhaustive search method described in [20] to solve (27). The numerical results are averaged over $20,000$ independent realizations of a network with the following parameters: $T_s = 89.28\mathrm{ns}$, $N = 1,024$, $M = 4$, $V = 36$, $\overline{\Pi}_{\mathrm{fa}} = 10^{-5}$, and $\overline{\mathrm{MSE}}_\theta = 324$, which yield $\rho = 128$, $\lambda = 0.12$, $\gamma_{\mathrm{req}} \mid_{\mathrm{dB}} = -6.19$, and $\gamma^\star \mid_{\mathrm{dB}} = \tilde{\gamma} \mid_{\mathrm{dB}} = 7.09$ (see [10] for a detail discussion on this parameter setting). The normalized power constraints are fixed to $\underline{p}/\sigma_n^2 \mid_{\mathrm{dB}} = -20$ and $\overline{p}/\sigma_n^2 \mid_{\mathrm{dB}} = +30$ for all k, whereas the ST distances d_k are

randomly chosen from a uniform distribution in $[R/10, R]$ with R being the cell radius. The channel power gains are normalized to a distance $R/2$ and are modeled using the 6-tap ITU modified vehicular-A model [21] with a path loss exponent $\varsigma = 2$.

Figure 1 reports the normalized MSE defined as $\mathrm{NMSE}(\mathbf{p}_c^\star) = \mathbb{E}\{\|\mathbf{p}_c^\star - \mathbf{p}_\Delta^\star\|^2/\|\mathbf{p}_c^\star\|^2\}$ as a function of K for different quantization steps, where $\mathbf{p}_c^\star$ is the unique GNE of $\mathcal{G}_c$. The maximum number of STs is fixed to $\lfloor 1 + V/\gamma^\star \rfloor = 8$. Observe that the condition $K \leq 8$ is required to meet (25). In addition, it represents a necessary and sufficient condition for the existence of the unique GNE $\mathbf{p}_c^\star$ [10]. As expected, $\mathrm{NMSE}(\mathbf{p}_c^\star)$ decreases as Δ becomes smaller since the discrete action sets $\mathcal{A}_k$ in $\mathcal{G}$ tend to better approximate the continuous ones in $\mathcal{G}_c$. As can be seen, $\mathrm{NMSE}(\mathbf{p}_c^\star)$ increases as K increases, meaning that the difference between $\|\mathbf{p}_\Delta^\star\|^2$ and $\|\mathbf{p}_c^\star\|^2$ becomes larger as the number of STs increases. In particular, we see that $\mathrm{NMSE}(\mathbf{p}_c^\star)$ is almost constant up to $K = 4$, whereas it rapidly increases for larger values.

To evaluate the impact of this difference on the system performance in terms of social welfare, Figure 2 reports the experimental $\sum_k u_k(\mathbf{p}_\Delta^\star)/\sum_k u_k(\mathbf{p}_c^\star)$ as a function of K in the same operating conditions of Figure 1. As seen, the ratio $\sum_k u_k(\mathbf{p}_\Delta^\star)/\sum_k u_k(\mathbf{p}_c^\star)$ is approximately 1 for $K \leq 6$ while it increases for larger values of K. A
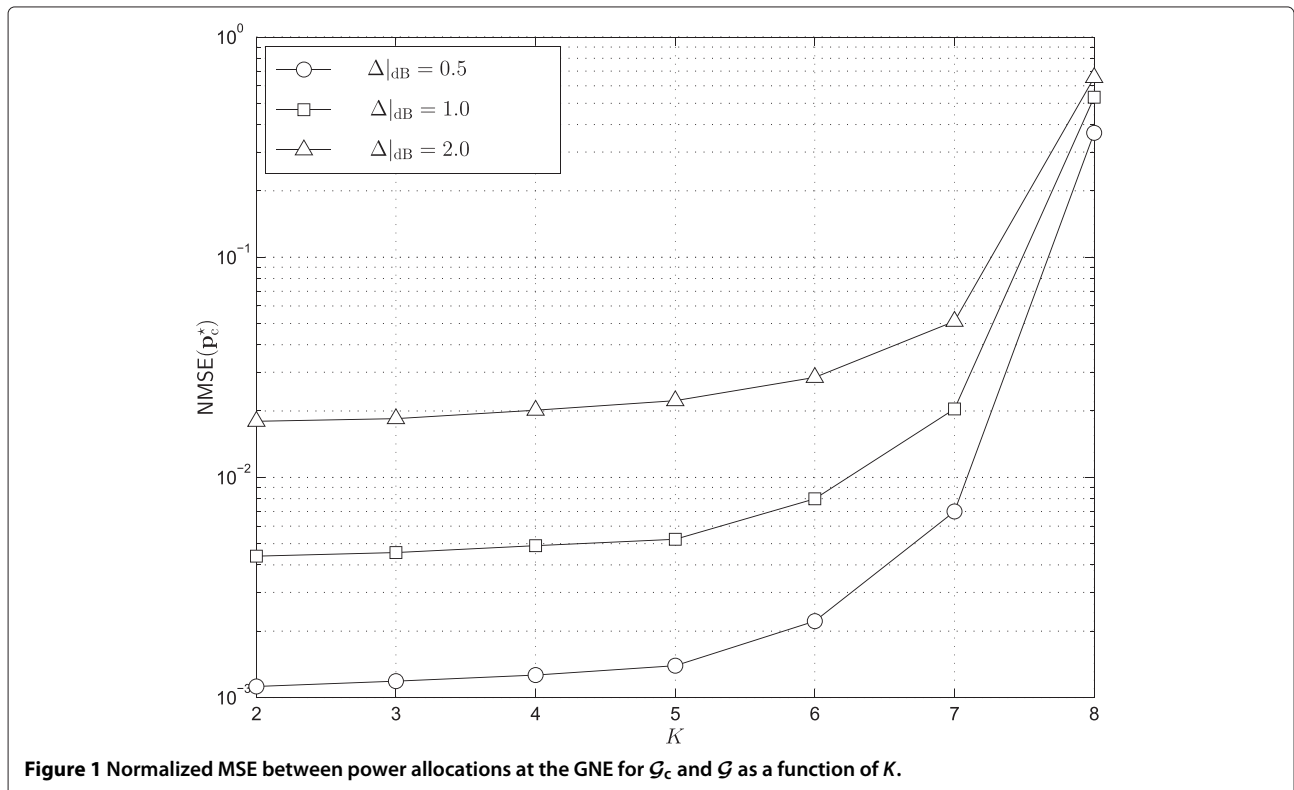
similar behavior (not shown for the sake of brevity) is observed if the user-basis ratio $u_k(\mathbf{p}_\Delta^\star)/u_k(\mathbf{p}_c^\star)$ is considered. From these results, it follows that limiting the STs to use a discrete set of strategies $\mathcal{A}_k$ increases the global system performance rather than introducing a detrimental effect. This phenomenon is known as a Braess-type paradox[g] [22], and it has already been observed in other different contexts (such as routing in [23,24] and wireless communications in [25,26]). Roughly speaking, the Braess-type paradox occurs because the average number of GNEs increases when K becomes larger. For example, when $\Delta |_{dB} = 1$, the numerical results indicate that the average number of GNE for $K = \{2, 3, 4, 5, 6, 7, 8\}$ is $\{1.0, 1.1, 1.2, 1.3, 1.7, 2.7, 20.9\}$, respectively. As mentioned before, the latter are found by solving (27) for each network realization by means of the exhaustive search procedure illustrated in [20].

4 Energy-efficient distributed synchronization
In what follows, we first show how to exploit the GNE analysis provided so far to derive a practical power control algorithm for achieving synchronization in a distributed manner. The performance of the provided solution is then investigated by means of numerical results.

4.1 Implementation of the algorithm
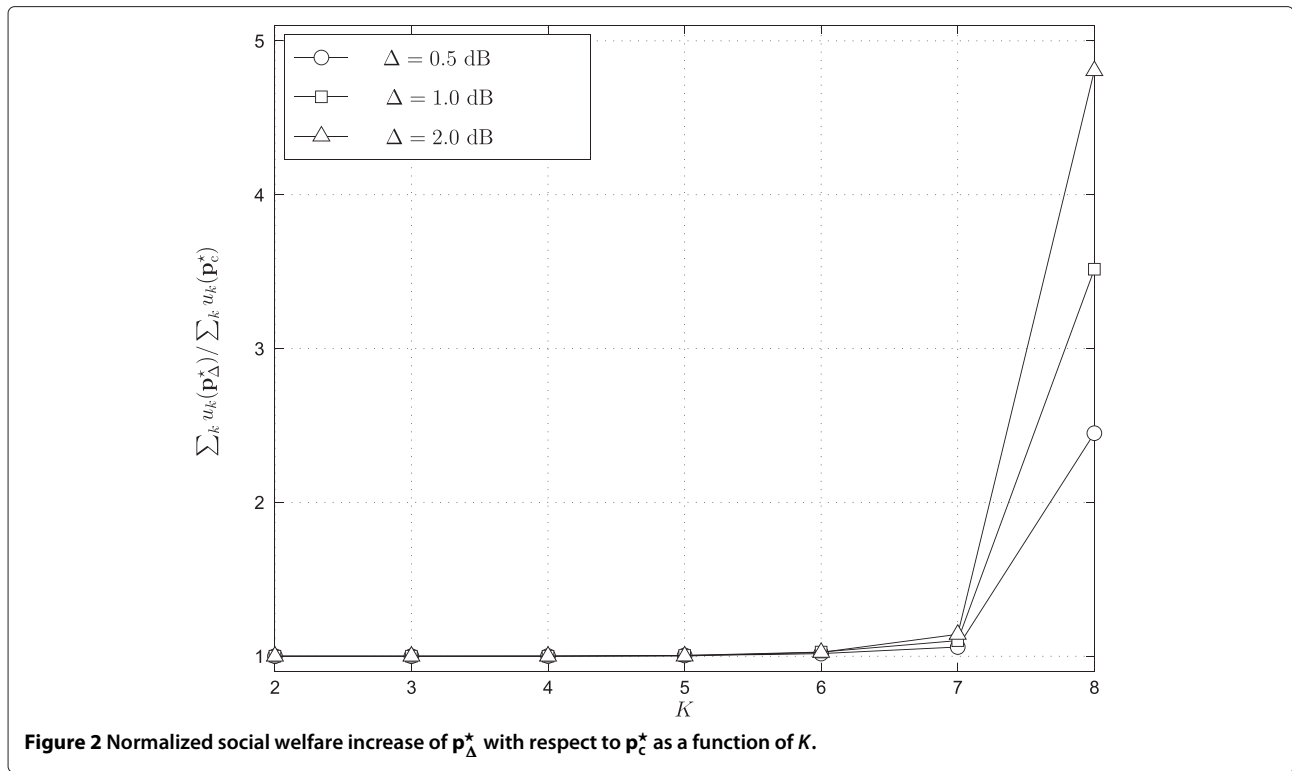We begin by observing the following result.

Figure 1 Normalized MSE between power allocations at the GNE for $\mathcal{G}_c$ and $\mathcal{G}$ as a function of K.

Figure 2 Normalized social welfare increase of $\mathbf{p}_\Delta^\star$ with respect to $\mathbf{p}_c^\star$ as a function of *K*.

Corollary 1. *If the powers of all active STs are initialized to the lowest levels $\underline{p}$, an iterative algorithm operating according to the best response dynamics given in* (22) *converges to $\mathbf{p}_\Delta^\star$ under the hypothesis* (25).

Proof. Since the best response dynamics reported in (22) possesses the *ascending* property [27] (see Appendix 1), using [28] the thesis follows. □

Denote by $p_k[n]$ the transmit power of the kth ST at the nth iteration step. Using Corollary 1, it follows that an iterative algorithm operating according to the best response dynamics in (22):

$$p_k[n+1] = \arg\max_{\tilde{p}_k \in \mathcal{A}_k} \frac{\Pi_{\mathrm{d},k}\left(\nu_k(\mathbf{p}_{\backslash k}[n])\tilde{p}_k\right)}{\tilde{p}_k T} \tag{28}$$

converges to the most socially efficient GNE $\mathbf{p}_\Delta^\star$ if $p_k[0] = \underline{p}$ for $k = 1, 2, \ldots, K$.

Note that the computation of $p_k[n+1]$ in (28) requires knowledge of $\nu_k(\mathbf{p}_{\backslash k}[n])$. Using (9), it follows that $\nu_k(\mathbf{p}_{\backslash k}[n])$ can be obtained as

$$\nu_k(\mathbf{p}_{\backslash k}[n]) = \frac{\gamma_k[n]}{p_k[n]} \tag{29}$$

where $\gamma_k[n]$ is ST k's SINR measured at the BS at time step n. While $p_k[n]$ is locally available at the transmitter, $\gamma_k[n]$

can only be estimated at the BS and sent to the kth ST on a downlink control channel. Following [10], an unbiased estimate $\hat{\gamma}_k[n]$ of $\gamma_k[n]$ can be computed as

$$\hat{\gamma}_k[n] = \frac{V\Lambda_k(\hat{\theta}_k) - \sum_{m=0}^{M-1}\|\mathbf{X}(m)\|^2}{\sum_{m=0}^{M-1}\|\mathbf{X}(m)\|^2 - \Lambda_k(\hat{\theta}_k)}. \tag{30}$$

To reduce the amount of information to be exchanged, we assume the quantity $\hat{\gamma}_k[n]$ to be quantized on a logarithmic scale using a uniform B-bit quantizer. This produces

$$\mu_k[n]\,|_{\mathrm{dB}} = \Delta_\gamma\,|_{\mathrm{dB}} \cdot b_k[n] \tag{31}$$

where

$$b_k[n] = \left\lfloor \frac{\left(\left[\hat{\gamma}_k[n]\right]_{\underline{\gamma}}^{\overline{\gamma}} - \underline{\gamma}\right)\Big|_{\mathrm{dB}}}{\Delta_\gamma\,|_{\mathrm{dB}}} \right\rceil \tag{32}$$

and

$$\Delta_\gamma\,|_{\mathrm{dB}} = \frac{\overline{\gamma}\,|_{\mathrm{dB}} - \underline{\gamma}\,|_{\mathrm{dB}}}{2^B - 1} \tag{33}$$

is the quantizer resolution (also known at the ST side, e.g., selected by the system standard), with $\overline{\gamma}$ and $\underline{\gamma}$ being the maximum and minimum expected values for $\hat{\gamma}_k[n]$, respectively. The BS sends on a broadcast downlink channel the integer $b_k[n]$, which is used by the kth ST to retrieve the quantized version of $\hat{\gamma}_k[n]$ using (31).

Replacing $\gamma_k[n]$ with $\mu_k[n]$ into (29) and substituting the result into (28), we eventually obtain

$$p_k[n+1] = \arg \max_{\tilde{p}_k \in \mathcal{A}_k} \frac{\Pi_{\mathrm{d},k}\left(\mu_k[n]\,\tilde{p}_k/p_k[n]\right)}{\tilde{p}_k T}. \qquad (34)$$

Recalling (31), it follows that its evaluation at the ST side requires only the knowledge of $b_k[n]$.

Algorithm 1 Discrete and limited feedback best response synchronization algorithm (DLF-BRSA)

---

a. *Initialization:* each ST $k = 1, 2, \ldots, K$

    a1. initializes the transmit power $p_k[0]$ to the lowest power value $\underline{p}$;
    a2. sets $n = 0$.

b. *Iterative algorithm:* at each step n, each ST k

    b1. receives on a common downlink channel the result of the GLRT (3) for code $\mathbf{c}_k$ and the integer $b_k[n]$ computed through (30)–(33);
    b2. if the GLRT for code $\mathbf{c}_k$ is verified and $\mu_k[n] > \gamma_{\mathrm{req}}$, exits the algorithm (i.e., ST k is successfully associated to the BS), otherwise goes to the next step;
    b3. adjusts its transmit power according to (34);
    b4. updates $n = n + 1$.

Collecting all the above facts together leads to the energy-efficient synchronization algorithm illustrated in Algorithm 1, which allows each ST to operate in a complete distributed manner without any knowledge of other users' power allocation strategies (as if in a single-user scenario).

Observe that Algorithm 1 is reminiscent of the best response synchronization algorithm (BRSA) illustrated in [10], except for the discrete action sets and the limited feedback from the BS, which makes it more suited for a practical implementation. In the sequel, we call the iterative procedure described in Algorithm 1 as discrete and limited feedback best response synchronization algorithm (DLF-BRSA).

Remark 1. An iterative algorithm using (28) as the power update criterion using $\gamma_k[n]$, $p_k[0] = \underline{p}$ for all STs k, without the exit condition on the GLRT converges to $\mathbf{p}_\Delta^\star$, as confirmed by Corollary 1. However, for a practical implementation, Algorithm 1 introduces (a) estimated SINRs $\hat{\gamma}_k[n]$, (b) limited feedback $b_k[n]$, and (c) the exit condition on the GLRT (step b2). These modifications affect the performance of the algorithm, and their impact will be studied in Section 4.2. Note that the minimum power initialization (step a2) is expedient to avoid the

maximum power constraint $\bar{p}_k$ to be violated for some steps n of the algorithm.

Remark 2. It is worth observing that, in their most basic forms, iterative algorithms based on best response dynamics require a significant amount of information to be locally available at the player (transmitter) [29]. For example, they usually require knowledge of the number of players and of the actions played by all the other players. To overcome this problem, other algorithms based on reinforcement learning techniques have been adopted in the literature [29]. The main advantage of these solutions is that they do require each player to know only its corresponding utility. Although based on best response dynamics, DLF-BRSA possesses most of the advantages shown by other reinforcement learning-based algorithms, as it allows each ST to operate in a distributed and iterative way requiring only knowledge of its own estimated SINR, as illustrated in Algorithm 1 by means of simulation results.

Remark 3. Most of the computational complexity of DLF-BRSA is represented by the exhaustive search in (34), which must be performed at each iteration step n over the Q discrete power levels of the set $\mathcal{A}_k$. In those applications characterized by large values of Q, this may represent an implementation impairment. In such cases, one may resort to the supermodularity properties of the utility function u_k (see Appendices 1 and 2) and reduce the search complexity looking only at the values of $\tilde{p}_k \in \mathcal{A}_k$ in the neighborhood of $p_k[n]$.

4.2 Simulation results

Numerical simulations are now used to assess the performance of DLF-BRSA and to make comparisons with existing alternatives. As in Section 3.2, the numerical analysis is conducted by averaging over $20,000$ independent realizations of a network whose parameters are fixed as follows: $T_s = 89.28\,\mathrm{ns}$, $N = 1,024$, $M = 4$, $V = 36$, $\overline{\Pi}_{\mathrm{fa}} = 10^{-5}$, and $\overline{\mathrm{MSE}}_\theta = 324$, which yield $\rho = 128$, $\lambda = 0.12$, $\gamma_{\mathrm{req}}\;|_{\mathrm{dB}} = -6.19$, and $\gamma^\star\;|_{\mathrm{dB}} = \tilde{\gamma}\;|_{\mathrm{dB}} = 7.09$. The minimum and maximum expected values of $\hat{\gamma}_k[n]$ in (33), based on an extensive simulation campaign, are fixed to $\underline{\gamma}\;|_{\mathrm{dB}} = -8$ and $\overline{\gamma}\;|_{\mathrm{dB}} = +16$, whereas the appropriate number of bits B is chosen later on the basis of the following numerical analysis. Without loss of generality, we concentrate on the first ST (i.e., $k = 1$) and assess the performance of the investigated solutions when its distance d_1 is kept constant. All other STs are assumed to be randomly located in $[R/10, R]$ with R being the cell radius. The normalized power constraints are fixed to $\underline{p}/\sigma_n^2\;|_{\mathrm{dB}} = -20$ and $\bar{p}/\sigma_n^2\;|_{\mathrm{dB}} = +30$, and the same power initialization $p_k[0] = \underline{p}$ is used for all STs $k \in \mathcal{K}$, which also use a common power quantization step $\Delta\;|_{\mathrm{dB}} = 1$.

Figure 3 reports the average normalized power expenditure p_{avg}/σ_n^2 (in dB) required by ST 1 when using DLF-BRSA, from the time it accesses the network until it successfully completes the synchronization procedure. The numerical results are plotted as functions of K for $B = \{1, 2, 3, 8\}$. The results obtained with DLF-BRSA when $B \to \infty$ (i.e., with continuous SINR feedback) are used as a benchmark. Comparisons are also made with the BRSA illustrated in [10] in which the action sets are continuous and perfect knowledge of the estimated SINRs is available at the STs. The results of Figure 3 indicate that the quantization of the SINRs has only a marginal effect on the performance of DLF-BRSA. In fact, it has practically the same performance for $B = 3, 8$ and $B \to \infty$, whereas a significant degradation is observed only for $B = 1$. We argue that the quantization of the estimated SINRs marginally impacts the system performance since it is basically perceived at the STs as an additional estimation error introduced by the BS (which, on the other hand, can actually exploit real-valued estimation methods). Based on the above results, in all subsequent simulations, we set $B = 3$. From (33), recalling that $\underline{\gamma} \mid_{dB} = -8$ and $\overline{\gamma} \mid_{dB} = +16$, we have $\Delta_\gamma \mid_{dB} = 3.43$.

To evaluate the impact of the discretization of the action sets, we now compare the performance of BRSA with that of DLF-BRSA. From Figure 3, it follows that they do perform identically when the DLF-BRSA uses $B \geq 3$. This seems to contradict the numerical results of Figure 2, discussed at the end of Section 3.2, which show that discretizing the set of strategies is beneficial for individual (and, consequently, global) performance. On the basis of the analysis of Section 3.2, the DLF-BRSA is expected to outperform the BRSA. The motivation behind this contradictory result can be understood by recalling that the considered ST takes part in the synchronization procedure as long as it is not correctly detected by the BS. As a consequence, what really impacts on the performance of DLF-BRSA and BRSA is its power evolution from the time it enters the network ($n = 0$) to the time step n^{exit} in which the exit conditions (detailed in step b2 of DLF-BRSA) are satisfied.

To this aim, Figure 4 reports the average number of iterations n_{avg}^{exit} as a function of K, which turns out to be the same for the both the BRSA and the DLF-BRSA (with $B \geq 3$) with good approximation. Interestingly, numerical simulations confirm that, when $0 \leq n \leq n^{exit}$, the difference between the power updates across the two schemes is negligible. On the contrary, the performance measured in Figure 2 corresponds to that achieved by the BRSA and the DLF-BRSA schemes *without* the exit conditions listed in step b2 (as the GNE, computed in Section 3.2 through an exhaustive search [20], can also be achieved using the best response dynamics described in Section 4), whose convergence time is usually much higher than n^{exit}. This is the reason why the performance in terms of total energy expenditure reported in Figure 3 is similar in the two cases. On the basis of the above results, we can conclude that DFL-BRSA yields the same
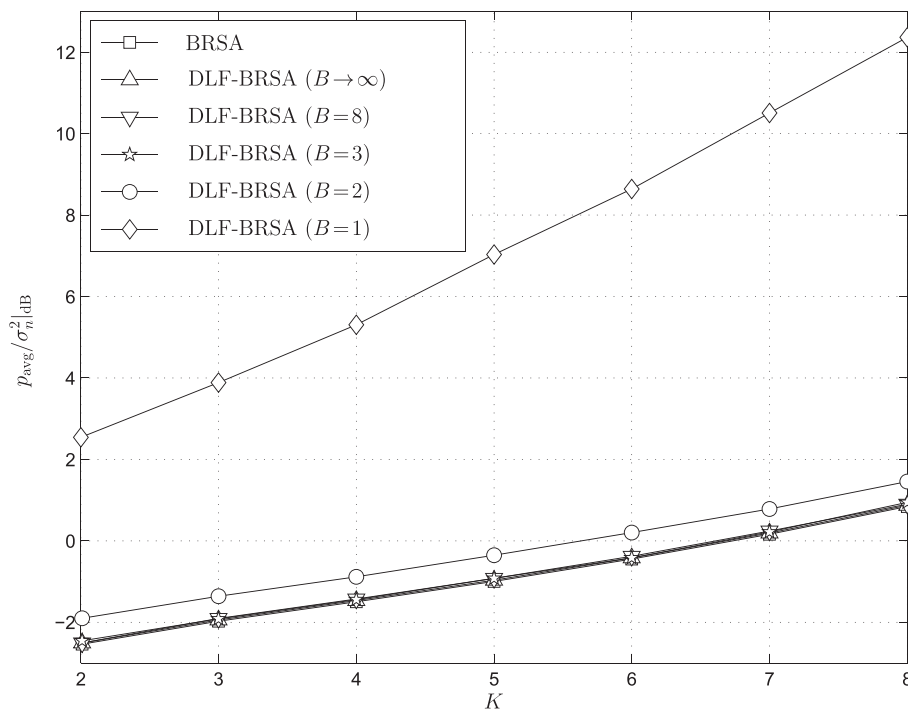

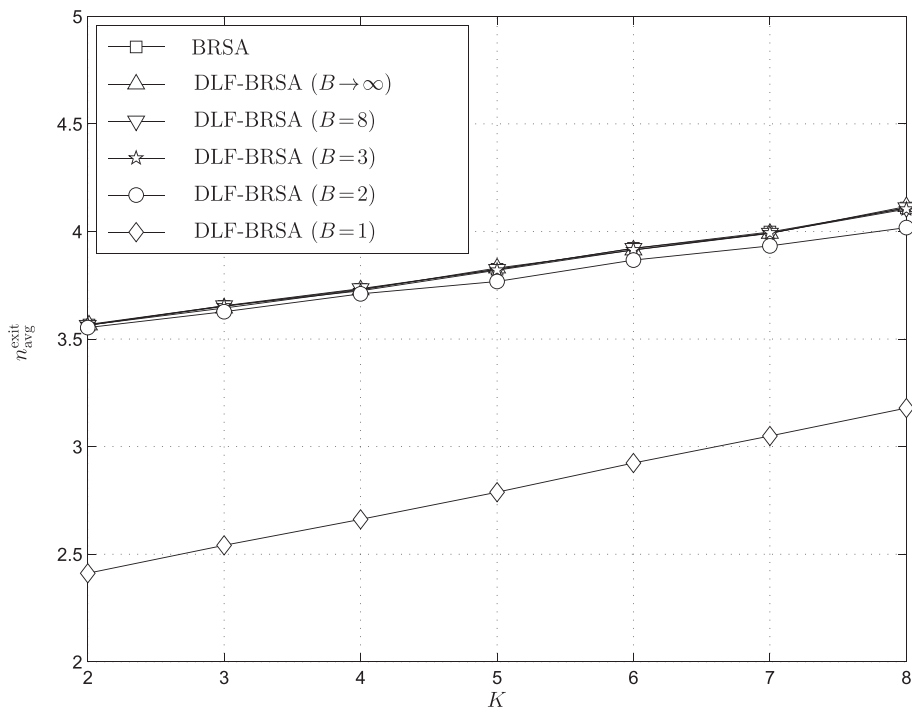**Figure 3 Average power consumption as a function of the number of STs.**

Figure 4 Average number of iterations as a function of the number of STs.

performance of BRSA. However, this is achieved while (a) reducing the complexity of the user terminals (thanks to the discretization of the power amplifier) and (b) requiring a limited amount of feedback from the BS (thanks to the finite number of bits B used to send the estimated SINRs).

The performance of DLF-BRSA is now compared with those achieved by two alternative solutions based on a deterministic increase of the transmit power: the deterministic synchronization algorithm (DSA), in which the update rule is $p_k[n+1] \mid_{dB} = p_k[n] \mid_{dB} + \Delta \mid_{dB}$, and the binary exponential backoff DSA (BEB-DSA), in which $p_k[n+n_e] \mid_{dB} = p_k[n] \mid_{dB} + \Delta \mid_{dB}$, where n_e is an exponentially distributed backoff counter (see [10] for more details). In all subsequent simulations, we set $\Delta \mid_{dB} = 1$ and $p_k[0] = \underline{p}$ for $k = 1, 2, \ldots, K$.

Figure 5 shows p_{avg}/σ_n^2 for all investigated solutions as a function of the normalized distance d_1/R when $K = 5$, and Figure 6 illustrates the average time T_{avg} needed to complete the synchronization procedure in the same operating conditions. In particular, T_{avg} is computed as $T_{avg} = T_f \cdot n_{avg}^{exit}$, where $T_f = 5$ ms accounts for the time interval (frame time) between two successive synchronization attempts. In addition, Figure 7 shows the MSE of the timing estimate $\hat{\theta}_1$ in the same simulation setup of Figures 5 and 6. From the results of Figure 5, it follows that DLF-BRSA provides roughly the same power consumption of BEB-DSA, which is

significantly lower than that needed by DSA. However, the results of Figure 6 show that the time required by DLF-BRSA to achieve synchronization is much shorter than that needed by DSA and BEB-DSA, especially when d_1/R increases. In addition, Figure 7 shows that the estimation accuracy with DLF-BRSA is higher than that with both DSA and BEB-DSA. Note also that simulation results (not reported here for the sake of brevity) show that the performance of the DLF-BRSA does not change as a function of $\bar{p}_k$ provided that $\bar{p}_k \gg \sigma_n^2$, whereas the average synchronization time achieved by the deterministic increase techniques (especially the DSA) increases as $\bar{p}_k$ increases. This is due to the fact that in this case colliding users transmit at comparable power levels for a longer time.

Similar conclusions can be drawn in the case of a variable number of STs K, by comparing the performance in terms of average synchronization time achieved by the DLF-BRSA (obtained by scaling the average number of iterations of Figure 4 by the frame interval T_f) with that provided by the DSA and the BEB-DSA [10, Figure eleven]. Since the slope of the curve provided by the DLF-BRSA, which scales linearly with K, is always lower that that achieved by a deterministic power increase, we can conclude that the proposed solution is particularly suitable when users are required to be synchronized in a short time interval with a limited amount of power.
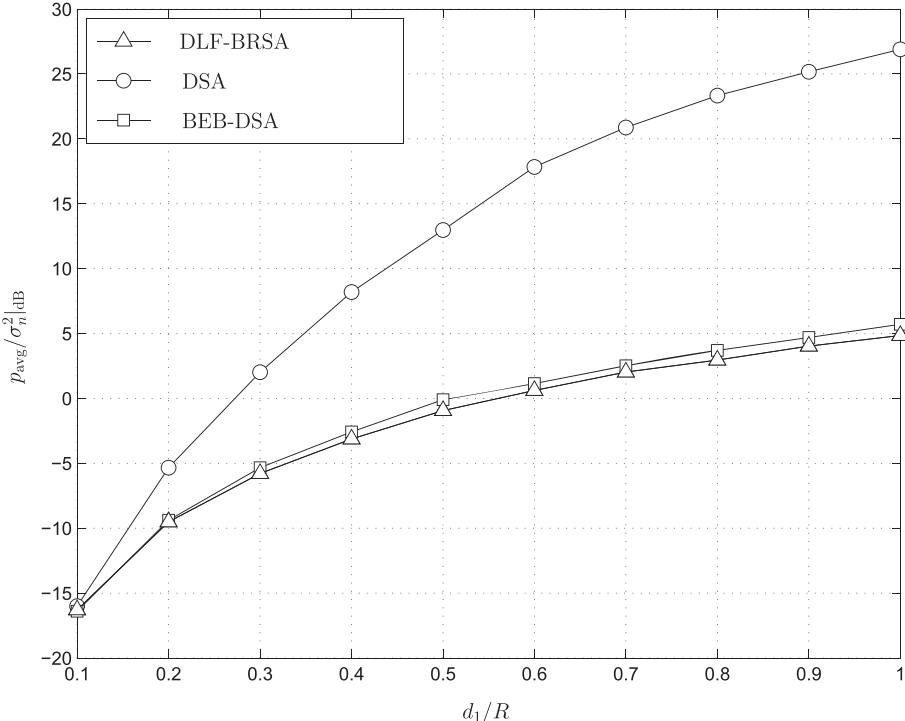
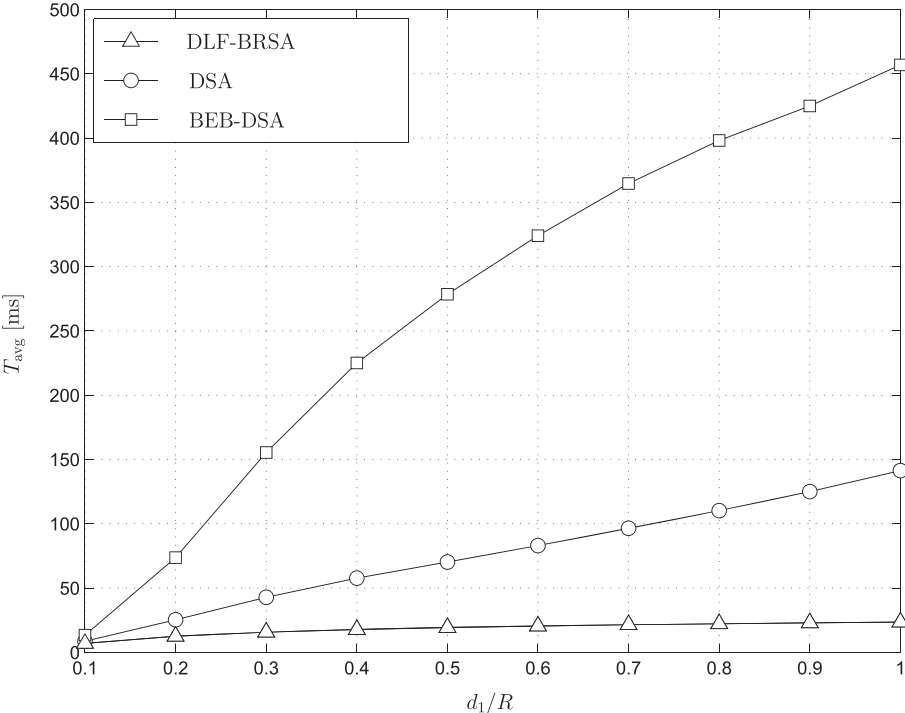**Figure 5 Average power consumption as a function of the normalized distance.**

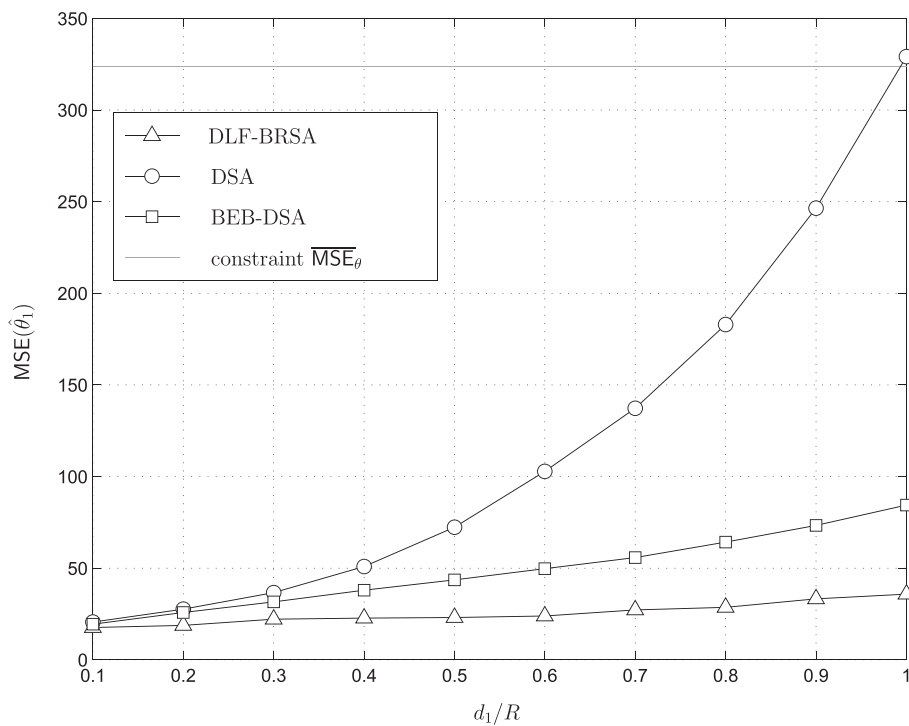**Figure 6 Average synchronization time as a function of the normalized distance.**

Figure 7 Average timing MSE as a function of the normalized distance.

Collecting all the above facts together, we may conclude that DLF-BRSA provides better results in terms of *energy efficiency* and *parameter estimation accuracy*, also providing some performance that slightly depends on the transmitter-receiver distance. This is achieved at the price of a slight increase of information to be fed back over the control channel. In particular, the amount of information to be exchanged during each frame and for each $\mathbf{c}_\ell \in \mathcal{C}$ is the following: 1 bit to broadcast the outcome of the GLRT and $B = 3$ bits to transmit the quantized SINRs. This means that a total of $4|\mathcal{C}|$ bits per frame time T_f is required by DLF-BRSA, which corresponds to a feedback rate on the order of a few tens of kilobits per second, given that $|\mathcal{C}|$ is usually on the order of tens to hundreds (e.g., see [2,3]).

5 Conclusion

In this work, we have formalized the power allocation problem for energy-efficient contention-based synchronization in OFDMA-based networks as a finite constrained noncooperative game. The generalized Nash equilibria have been analytically studied and numerically evaluated. The above results have been used to derive a distributed and iterative energy-efficient power control algorithm with discrete powers and limited feedback. The performance of the above solution has been evaluated and compared with alternatives by means of

numerical simulations. Using realistic system parameters and widely agreed-upon channel models, we have shown that the proposed solution incurs only a negligible degradation with respect to the scheme illustrated in [10], while a significant gain is achieved with respect to deterministic-based power allocation approaches (both with and without contention resolution methods). The derived technique requires a feedback on the downlink on the order of a few tens of kilobits per second, which can be easily accommodated in current IEEE 802.16 m [2] and LTE [3] standards. Since the proposed solution shows a (much) faster synchronization time than deterministic methods, it can be used to further increase the energy efficiency of mobile terminals by reducing the frequency of periodic ranging procedures, which are currently used by 4G communication systems to meet the transmission latency requirements.

Endnotes

[a] The following notation is used throughout the paper. Matrices and vectors are denoted by boldface letters. $\mathbf{I}_n$, $\mathbf{0}_n$, and $\mathbf{1}_n$ are the $n \times n$ identity matrix, the $n \times 1$ all-zero vector, and the $n \times 1$ all-one vector, respectively, whereas $\mathbf{A} = \text{diag}\{a(n) \,; \, n = 1, 2, \ldots, N\}$ denotes an $N \times N$ diagonal matrix with entries $a(n)$ along its main diagonal. We use $\mathbb{E}\{\cdot\}$, $(\cdot)^T$, and $(\cdot)^H$ for expectation, transposition,

and Hermitian transposition, respectively; $\|\cdot\|$ for the Euclidean norm of the enclosed vector; $\lfloor x \rfloor$ to round x to the nearest integer towards zero; $\lfloor x \rceil$ to round x to the nearest integer; $x\,|_{\mathrm{dB}} = 10 \log_{10} x$; and finally, $[x]_a^b = \max(a, \min(x, b))$.

[b] This assumption is reasonable as long as downlink estimation errors are within a few percents of the subcarrier spacing and low mobility applications are considered [2].

[c] In practice, it suffices that $\overline{p}_k$ is at least a couple of orders of magnitude larger than the AWGN power σ_n^2, which is normally verified in all communication standards.

[d] The game is generalized since $\mathcal{A}_k$ depends on the other STs' power $\mathbf{p}_{\setminus k}$ (see, for example, [14] and [30] for more details).

[e] Please note that, following the steps reported in Appendix 1, the maximum power constraint is active when deriving (25).

[f] The smallest vector in a set of vectors refers to the component-wise comparison between vectors in that set. For example, for any two vectors $\mathbf{x}, \mathbf{y} \in \mathbb{R}^n$, $\mathbf{x} < \mathbf{y}$ if and only if $x_i < y_i$ for all $i = 1, 2, \ldots, n$.

[g] Braess's paradox states that adding extra strategies to a network when the entities operate selfishly can, in some cases, reduce the overall performance. This is because the Nash equilibrium of such system is not necessarily optimal. In the problem at hand, this means that relying on continuous power sets does not necessarily bring benefits to the synchronization procedure due to the inefficiency of the unique Nash equilibrium of the continuous-power game.

Appendices
Appendix 1
Proof of Theorem 1

Figure 8 shows a pictorial representation of the typical shape of the utility $u_k(\mathbf{p})$ as a function of the power $p_k = \pi_k^{(q)}$ for a fixed interference $\mathbf{p}_{\setminus k}$ (all quantities are on a logarithmic scale, although the subscript 'dB' is suppressed for the sake of presentation). The relevant points of the utility function in terms of SINR, scaled by the quantity $\nu_k(\mathbf{p}_{\setminus k})$, are also reported: in addition to γ_{req} and $\tilde{\gamma}$, defined in (17) and (24), respectively, Figure 8 also shows the inflection point $\dot{\gamma}$, $\dot{\gamma} < \tilde{\gamma} \leq \gamma^\star$, such that $\Pi_{\mathrm{d},k}(\gamma_k)$ is strictly convex for $\gamma_k < \dot{\gamma}$ and strictly concave for $\gamma_k > \dot{\gamma}$. It is worth observing that $\dot{\gamma}$ is easily found from (13). Although Figure 8 depicts the case $\gamma_{\mathrm{req}} < \tilde{\gamma}$, the considerations drawn in the following apply in the case $\gamma_{\mathrm{req}} \geq \tilde{\gamma}$ as well. Circular markers report $u_k([\pi_k^{(q)}, \mathbf{p}_{\setminus k}])$ for $q = 1, \ldots, Q$ (in this example, $Q = 8$). Note that the best response map defined in (22) may yield $r_k(\mathbf{p}_{\setminus k}) < \gamma^\star/\nu_k(\mathbf{p}_{\setminus k})$, as occurs in this example.

A GNE in the game $\mathcal{G}$ exists provided that the K sets $\mathcal{A}_k(\mathbf{p}_{\setminus k}) \subseteq \mathcal{P}_k$, $k \in \mathcal{K}$, are nonempty, which translates, using (19), into ensuring that there exists at least a power level $\pi_k^{(q)} \in \mathcal{P}_k$ such that $\pi_k^{(q)} \geq \gamma_{\mathrm{req}}/\nu_k(\mathbf{p}_{\setminus k})$ for all k. Since $\gamma_{\mathrm{req}} \leq \gamma^\star$ by hypothesis, it is sufficient to show that $\gamma^\star/\nu_k(\mathbf{p}_{\setminus k}^\star) \leq r_k(\mathbf{p}_{\setminus k}^\star) = p_k^\star \leq \overline{p}_k$ for all $k \in \mathcal{K}$. By following the same steps as in [11], we can derive the sufficient condition (25), which becomes also necessary in the case $\gamma^\star = \gamma_{\mathrm{req}}$. Note that, unlike [11], here we cannot derive a necessary condition that holds for any $\tilde{\gamma} > \gamma_{\mathrm{req}}$, because of the inequality $\gamma^\star/\nu_k(\mathbf{p}_{\setminus k}) \leq r_k(\mathbf{p}_{\setminus k})$ that is originated from using a finite set, and hence, GNE might exist even though (25) is not fulfilled. This is also in accordance to what is highlighted in (22), as an equilibrium can exist even if $p_k^\star < \gamma^\star/\nu_k(\mathbf{p}_{\setminus k}^\star)$, provided that $\gamma^\star > \gamma_{\mathrm{req}}$.
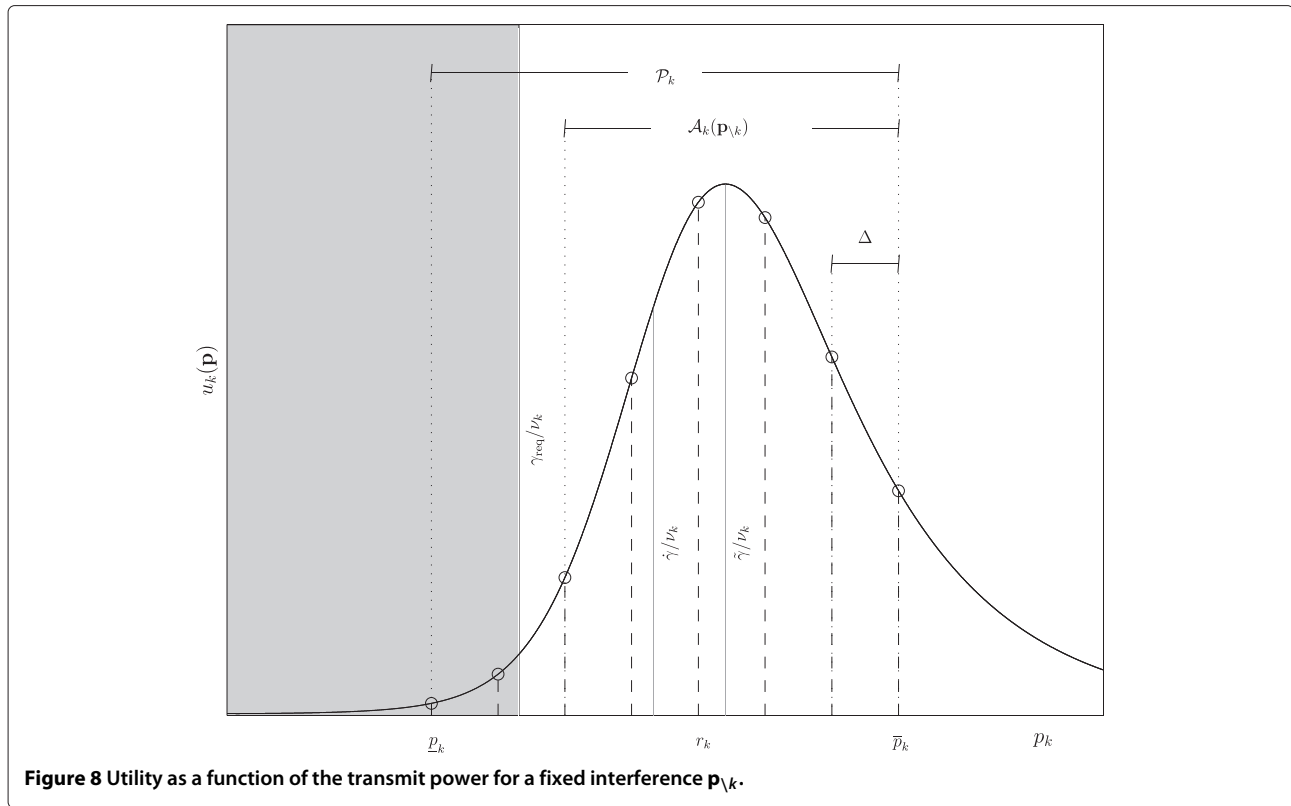
To proceed further with the proof of existence, it is useful to introduce the following definition:

Definition 1 ([27]). A best response $r_k(\mathbf{p}_{\setminus k})$ possesses the *ascending property* if $r_k(\mathbf{p}_{\setminus k}) \leq r_k(\mathbf{p}'_{\setminus k})$ for all $k \in \mathcal{K}$ when $\mathbf{p}_{\setminus k} \neq \mathbf{p}'_{\setminus k}$ is such that $p_\ell \leq p'_\ell \ \forall \ell \neq k$.

To show that the best response (22) is ascending, let us define $r_k = r_k(\mathbf{p}_{\setminus k})$, $r'_k = r_k(\mathbf{p}'_{\setminus k})$, $\nu_k = \nu_k(\mathbf{p}_{\setminus k})$, and $\nu'_k = \nu_k(\mathbf{p}'_{\setminus k})$ for notational convenience. Note that assuming $\mathbf{p}_{\setminus k} \neq \mathbf{p}'_{\setminus k}$ with $p_\ell \leq p'_\ell \ \forall \ell \neq k$ implies that $\nu_k > \nu'_k$. Let us consider two different cases:

1. $r_k < \gamma^\star/\nu_k$: in this domain, $u_k([p_k, \mathbf{p}'_{\setminus k}])$ is an increasing function of p_k. Hence, power vector $\mathbf{p}'_{\setminus k}$'s best response is $r'_k = \arg\max_{p_k} u_k([p_k, \mathbf{p}'_{\setminus k}]) \geq r_k$.

2. $r_k \geq \gamma^\star/\nu_k$: in this domain, since $\nu_k > \nu'_k$, both $u_k([p_k, \mathbf{p}_{\setminus k}])$ and $u_k([p_k, \mathbf{p}'_{\setminus k}])$ are decreasing functions of p_k. Hence, for r_k to be a best response, the condition $u_k([r_k, \mathbf{p}_{\setminus k}]) > u_k([r_k/\Delta, \mathbf{p}_{\setminus k}])$ must hold, with $r_k/\Delta < \gamma^\star/\nu_k$. Due to the asymmetry of $u_k([p_k, \mathbf{p}_{\setminus k}])$ with respect to the point of maximum $\gamma^\star/\nu_k$, $r_k/\Delta < \check{p}_k$, where $\check{p}_k$, $2\gamma^\star/\nu_k - r_k < \check{p}_k < \gamma^\star/\nu_k < \gamma^\star/\nu'_k$, is the power level such that $u_k([\check{p}_k, \mathbf{p}_{\setminus k}]) = u_k([r_k, \mathbf{p}_{\setminus k}])$. Since $u_k([p_k, \mathbf{p}'_{\setminus k}])$ is increasing in the region $p_k < \gamma^\star/\nu'_k$, $u_k([\check{p}_k, \mathbf{p}_{\setminus k}]) < u_k([\check{p}'_k, \mathbf{p}_{\setminus k}])$, where $\check{p}'_k > \check{p}_k$ is the counterpart power on $u_k([p_k, \mathbf{p}'_{\setminus k}])$ such that $u_k([\check{p}'_k, \mathbf{p}'_{\setminus k}]) = u_k([r_k, \mathbf{p}'_{\setminus k}])$, where the inequality $\check{p}'_k > \check{p}_k$ follows from the fact the maximum of $u_k([p_k, \mathbf{p}'_{\setminus k}])$ is placed at $\gamma^\star/\nu'_k > \gamma^\star/\nu_k$. Hence, $u_k([r_k/\Delta, \mathbf{p}_{\setminus k}]) < u_k([\check{p}'_k, \mathbf{p}'_{\setminus k}]) = u_k([r_k, \mathbf{p}'_{\setminus k}])$, which implies that $r'_k = r_k$.

As a conclusion, $r_k(\mathbf{p}_{\setminus k})$ is an ascending best response function. In particular, if (25) is satisfied, this implies that $r_k(\mathbf{p}_{\setminus k}) \geq r_k(\dot{\mathbf{p}}_{\setminus k})$ for all k and for all $\mathbf{p}$ such that

Figure 8 Utility as a function of the transmit power for a fixed interference $\mathbf{p}_{\backslash k}$.

$p_k \geq \dot{p}_k$, where the vector $\dot{\mathbf{p}} = [\dot{p}_1, \ldots, \dot{p}_K]^T$ is the minimum component-wise power allocation such that $\gamma_k = v_k(\dot{\mathbf{p}}_{\backslash k})\dot{p}_k \geq \dot{\gamma}$ for all $\dot{p}_k$, with $\dot{\gamma} < \tilde{\gamma}$ defined above. In other words, the equilibrium points of $\mathcal{G}$ (if any) are equal to the equilibria of a modified (generalized) game, which differs from $\mathcal{G}$ as now the strategy space is the subset of $\mathcal{P}_k$ such that any vector allocation $\mathbf{p}$ is such that $p_k \geq \dot{p}_k$, and hence, $\gamma_k \geq \dot{\gamma}$. To conclude the proof, let us introduce the following definition:

Definition 2 ([14,31]). A game is *supermodular* if $u_k(\mathbf{p})$ has increasing differences in $\mathbf{p} = [p_k, \mathbf{p}_{\backslash k}]$, i.e., if

$$u_k(\mathbf{p}) - u_k([p'_k, \mathbf{p}_{\backslash k}]) \geq u_k([p_k, \mathbf{p}'_{\backslash k}]) - u_k(\mathbf{p}') \quad (35)$$

for all $\mathbf{p}$ and $\mathbf{p}'$ such that, for all k, $p_k \leq p'_k$, and $p_\ell \leq p'_\ell$ for all $\ell \neq k$.

To prove that the utility $u_k(\mathbf{p})$, which is twice differentiable, satisfies (35), we can show, using [31], that it possesses the necessary and sufficient condition $\partial^2 u_k(\mathbf{p})/\partial p_\ell \partial p_k \geq 0$ for any two components $p_\ell \neq p_k$. Using (20), we can easily derive

$$\frac{\partial^2 u_k(\mathbf{p})}{\partial p_\ell \partial p_k} = -\frac{\alpha_\ell}{V\alpha_k} \cdot \frac{\Pi''_{\mathrm{d},k}(\gamma_k)\gamma_k^2 - 2f(\gamma_k)}{p_k^4} \geq 0 \quad (36)$$

where the inequality follows from the fact that $\Pi''_{\mathrm{d},k}(\gamma_k) = \partial^2 \Pi_{\mathrm{d},k}(\gamma_k)/\partial \gamma_k^2 \leq 0$ for $\dot{\gamma} \leq \gamma_k \leq \tilde{\gamma}$ and $f(\gamma_k) = \gamma_k \cdot \partial \Pi_{\mathrm{d},k}(\gamma_k)/\partial \gamma_k - \Pi_{\mathrm{d},k}(\gamma_k) > 0$ for $\gamma_k \leq \tilde{\gamma}$ (see [10,11] for further details). Proving the property of supermodularity concludes the proof, as supermodular games admit pure-strategy equilibria [14]. As a consequence, the original game $\mathcal{G}$ has pure-strategy GNE, under the sufficient condition (25).

Appendix 2
Proof of Theorem 2
To show that the GNE of the game $\mathcal{G}$ is not necessarily unique, we use a counterexample. Let us focus on one GNE $\mathbf{p}^\star$, whose existence is ensured by Theorem 1, and let us suppose that $\mathbf{p}^\star$ is such that $p_k^\star \leq \gamma^\star/(v'_k\sqrt{\Delta})$, where $v'_k = v_k(\mathbf{p}'_{\backslash k})$ is obtained using the vector $\mathbf{p}'_{\backslash k} = \Delta\mathbf{p}^\star$ such that all components are scaled by the quantization step Δ, i.e., $p'_k = \Delta p_k^\star$. Under this hypothesis, $\mathbf{p}'$ is also a GNE of $\mathcal{G}$, i.e., $r_k(\mathbf{p}'_{\backslash k}) = p'_k \ \forall k \in \mathcal{K}$.

To show this property, let us note first that $v_k^\star < v'_k < v_k^\star/\Delta$, where $v_k^\star = v_k(\mathbf{p}^\star_{\backslash k})$. Hence, if $p_k^\star \leq \gamma^\star/(v_k^\star\Delta)$ is the best response $p_k^\star = r_k(\mathbf{p}^\star_{\backslash k})$, it implies that $p'_k = \Delta p_k^\star \leq \gamma^\star/v'_k$ is also $p'_k = r_k(\mathbf{p}'_{\backslash k})$, as $|p'_k - \gamma^\star/v'_k| < |p_k^\star - \gamma^\star/v_k^\star|$ and $u_k([p_k, \mathbf{p}'_{\backslash k}])$ is an increasing function of p_k. If $\gamma'/(v_k^\star\Delta) < p_k^\star \leq \gamma'/(v_k^\star\sqrt{\Delta})$, then $\gamma'/v_k^\star < p'_k \leq$

$\gamma^\star \sqrt{\Delta}/v_k^\star$, i.e., $p_k' = \Delta p_k^\star$ is greater than the point of maximum $\gamma'/v_k^\star$. Furthermore, $|p_k' - \gamma^\star/v_k'| < |p_k^\star - \gamma^\star/v_k'|$. Due to the asymmetry of $u_k([p_k, \mathbf{p}'_{\backslash k}])$, this ensures that $u_k([p_k', \mathbf{p}'_{\backslash k}]) > u_k([p_k^\star, \mathbf{p}'_{\backslash k}])$, and thus, $p_k' = r_k(\mathbf{p}'_{\backslash k})$. As a conclusion, $\mathbf{p}' = \Delta \mathbf{p}^\star$ is also a GNE of $\mathcal{G}$, and this concludes the proof.

Note that, when $K \gg 1$ (e.g., $K = \lfloor 1 + V/\gamma^\star \rfloor$), it is often the case that $\sum_{\ell \neq k} \alpha_\ell p_\ell^\star \gg \sigma_n^2$, $\forall k$. Hence, $v_k' \gtrsim v_k^\star/\Delta$, and the condition $p_k^\star \leq \gamma^\star/(v_k'\sqrt{\Delta})$ occurs frequently. This is the reason why the number of GNE increases as K increases. However, such condition is not necessary, and other GNE might exist, e.g., vectors $\mathbf{p}'$ in which some elements are $p_k' = \Delta p_k^\star$ and some others are $p_k' = p_k^\star$.

Appendix 3
Proof of Theorem 3
By using relation (21), $u_k(\mathbf{p}_\Delta^\star) = u_k([p_{\Delta,k}^\star, \mathbf{p}_{\Delta,\backslash k}^\star]) \geq u_k([p_k, \mathbf{p}_{\Delta,\backslash k}^\star])$ for all k and for all $p_k \in \mathcal{P}_k$. In particular, $u_k([p_{\Delta,k}^\star, \mathbf{p}_{\Delta,\backslash k}^\star]) \geq u_k([p_k^\star, \mathbf{p}_{\Delta,\backslash k}^\star])$ for any $p_k^\star$ in any $\mathbf{p}^\star \in \mathcal{E}^\star$, $\mathbf{p}^\star \neq \mathbf{p}_\Delta^\star$. Note also that $\gamma_k' = v_k(\mathbf{p}_{\Delta,\backslash k}^\star)p_k^\star \geq v_k(\mathbf{p}_{\backslash k}^\star)p_k^\star = \gamma_k^\star$ for all k, and $\gamma_k' > \gamma_k^\star$ for some k, under the hypothesis $p_{\Delta,k}^\star \leq p_k^\star$ for all k, $\mathbf{p}_\Delta^\star \neq \mathbf{p}^\star$. As a consequence, $u_k([p_k^\star, \mathbf{p}_{\Delta,\backslash k}^\star]) = \Pi_{\mathrm{d},k}(\gamma_k')/p_k^\star \geq \Pi_{\mathrm{d},k}(\gamma_k^\star)/p_k^\star = u_k(\mathbf{p}^\star)$. Since $u_k(\mathbf{p}_\Delta^\star) \geq u_k(\mathbf{p}^\star)$ for all $k \in \mathcal{K}$, with strict inequality for some k, (27) follows.

References
1. H Zhang, A Gladisch, M Pickavet, Z Tao, W Mohr, Energy efficiency in communications. IEEE Commun. Mag. **48**(11), 48–49 (2010)
2. IEEE 80216 Broadband Wireless Access Working Group, *IEEE Standard for Local and Metropolitan Area Networks - Part 16: Air Interface for Broadband Wireless Access Systems - Amendment 3: Advanced Air Interface. Tech. Rep. IEEE 802.16m-2011* (IEEE Computer Society, Washington, 2011)
3. 3GPP Technical Specification Group, *LTE; Evolved Universal Terrestrial Radio Access (E-UTRA); Physical Channels and Modulation (Release 10). Tech. Rep. 3GPP TS 36.211 v. 10.4.0* (European Telecommunications Standards Institute, Sophia Antipolis, 2011)
4. X Fu, Y Li, H Minn, A new ranging method for OFDMA systems. IEEE Trans. Commun. **6**(2), 659–669 (2007)
5. M Ruan, M Reed, Z Shi, Successive multiuser detection and interference cancelation for contention based OFDMA ranging channel. IEEE Trans. Wireless Commun. **9**(2), 481–487 (2010)
6. L Sanguinetti, M Morelli, An initial ranging scheme for the IEEE 802.16 OFDMA uplink. IEEE Trans. Wireless Commun. **11**(9), 3204–3215 (2012)
7. L Sanguinetti, M Morelli, L Marchetti, A random access algorithm for LTE systems. Trans. Emerging Telecommun. Technol. **24**, 49–58 (2013)
8. G Miao, N Himayat, G Li, S Talwar, Distributed interference-aware energy-efficient power optimization. IEEE Trans. Wireless Commun. **10**(4), 1323–1333 (2011)
9. S Buzzi, G Colavolpe, D Saturnino, A Zappone, Potential games for energy-efficient power control and subcarrier allocation in uplink multicell OFDMA systems. IEEE J. Sel. Topics Signal Process. **6**(2), 89–103 (2012)
10. G Bacci, L Sanguinetti, M Luise, HV Poor, A game-theoretic approach for energy-efficient contention-based synchronization in OFDMA systems. IEEE Trans. Signal Process. **61**(5), 1258–1271 (2013)
11. G Bacci, M Luise, A game-theoretic perspective on code synchronization for CDMA wireless systems. IEEE J. Sel. Areas Commun. **30**, 107–118 (2012)
12. G Bacci, M Luise, A pre-Bayesian game for CDMA power control during network association. IEEE J. Sel. Topics Signal Process. **6**(2), 76–88 (2012)
13. G Bacci, Energy-efficient power control for CDMA code acquisition over frequency-selective channels. IEEE Commun. Lett. **16**(3), 364–367 (2012)
14. D Fudenberg, J Tirole, *Game Theory* (MIT Press, Cambridge, 1991)
15. M Morelli, Timing and frequency synchronization for the uplink of an OFDMA system. IEEE Trans. Commun. **52**(2), 296–306 (2004)
16. M Abramowitz, IA Stegun, *Handbook of Mathematical Functions* (Dover, New York, 1965)
17. S Lasaulce, H Tembine, *Game Theory and Learning in Wireless Networks: Fundamentals and Applications* (Academic, Oxford, 2011)
18. M Félegyházi, Non-cooperative behavior in wireless networks. PhD thesis, École Polytechnique Fédérale de Lausanne (EFPL), (2007)
19. S Lasaulce, M Debbah, E Altman, Methodologies for analyzing equilibria in wireless games. IEEE Signal Process. Mag. **26**(5), 41–52 (2009)
20. H Peyton Young, *Strategic Learning and its Limits* (Oxford University Press, Oxford, 2004)
21. ITU Radiocommunication Sector (ITU-R), *Guidelines for Evaluation of Radio Transmission Technologies for IMT-2000. Recommendation ITU-R M.1225* (International Telecommunication Union, Geneva, 1997)
22. SM Perlaza, Game theoretic approaches to spectrum sharing in decentralized self-configuring networks. PhD thesis, École Nationale Supérieure des Télécommunications, 2011
23. T Roughgarden, *Selfish Routing and the Price of Anarchy* (MIT Press, Cambridge, 2005)
24. E Altman, T Boulogne, R El Azouzi, T Jimenez, L Wynter, A survey on networking games in telecommunications. Comput. Oper. Res. **33**(2), 286–311 (2006)
25. E Altman, V Kamble, H Kameda, A Braess type paradox in power control over interference channels, in *Proc. Int. Symp. Modeling and Optimization in Mobile, Ad Hoc, and Wireless Networks,* Berlin, 1–3 Apr 2008
26. L Rose, SM Perlaza, M Debbah, On the Nash equilibria in decentralized parallel interference channels, in *Proc. IEEE Int. Conf. Commun.,* Kyoto, 5–9 June 2011
27. E Altman, Z Altman, S-modular games and power control in wireless networks. IEEE Trans. Autom. Control **48**(5), 839–842 (2003)
28. RD Yates, A framework for uplink power control in cellular radio systems. IEEE J. Sel. Areas Commun. **13**(9), 1341–1347 (1995)
29. L Rose, SM Perlaza, S Lasaulce, M Debbah, Learning equilibria with partial information in decentralized wireless networks. IEEE Commun. Mag. **49**(8), 136–142 (2011)
30. F Facchinei, C Kanzow, Generalized Nash equilibrium problems. Q. J. Oper. Res. **5**(3), 173–210 (2007)
31. DM Topkis, Equilibrium points in nonzero-sum n-person submodular games. SIAM J. Control Optimization. **17**(6), 773–787 (1979)